EPR and TPR investigation of the redox properties of vanadia based ceria catalysts

E. ABI-AAD*
Laboratoire de Catalyse et Environnement, E.A. 2598, Université du Littoral-Côte d'Opale, 145 Avenue Maurice Schumann, 59140, Dunkerque, France
E-mail: abiaad@univ-littoral.fr

J. MATTA
Institut de Recherche Industrielle, Campus Université Libanaise, Immeuble IRI, Hadath (Baabda), B.P. 11-2806, Beyrouth, Liban

D. COURCOT, A. ABOUKAÏS
Laboratoire de Catalyse et Environnement, E.A. 2598, Université du Littoral-Côte d'Opale, 145 Avenue Maurice Schumann, 59140, Dunkerque, France

Published online: 17 February 2006

Vanadium cerium oxides, with different V/Ce atomic ratios, were prepared using the impregnation method and calcined under air at 500°C. Physicochemical studies have shown that at low vanadium content, polymeric V-O-V chains are stabilized on the ceria surface. Increasing the vanadium content tends to favor the formation of the $CeVO_4$ and V_2O_5 phases. The redox properties of these oxides have been simultaneously investigated by TPR/TPO and EPR techniques. V-O-V chains and V_2O_5 species are more easily reducible than the $CeVO_4$ phase. The reduction of V_2O_5 to V_2O_3 proceeds in several steps, the intermediate species being V_6O_{13}, VO_2 and V_5O_9. The reduction of V_2O_5 species interacting with ceria support leads to VO oxide. EPR measurements performed at $T = -269$°C have permitted to observe progressively different signals of V^{4+} in addition to vanadium ions in V^{2+} ($3d^3$) paramagnetic configuration. This attribution is based on an EPR signal at $g = 3.956$ with eight well resolved hyper fine lines ($A = 96$ Gauss), which may be attributed to the perpendicular components of one of the fine transitions corresponding to the V^{2+} spectrum. At high reduction temperature, $CeVO_4$ phase leads in one step to $CeVO_3$ and a continuous and partial reduction of CeO_2 into Ce_2O_3 is observed. Re-oxidation process shows that polymeric V-O-V chains, easily reducible, are hardly re-oxidized whereas V_2O_5 species, present in the high vanadium loading samples, are easily re-oxidized at low temperatures. However, redox processes seem to be reversible.

1. Introduction

The CeO_2 and V_2O_5 oxides are commonly used as catalysts in the atmospheric cleaning reactions such as the oxidation of diesel soot particles. Vanadia (V_2O_5) based catalysts are proved to be quite effective for Selective Catalytic Reduction (SCR) of nitric oxide NO and also in different oxidation processes [1–2]. In parallel, ceria (CeO_2) has traditionally been used as a promoting component in the three way catalysts for automotive exhaust treatment. It exhibits a large deviation from its stoechiometric composition (CeO_{2-x}) making ceria a promising material for use either as a support or active catalyst in oxidation—reduction reactions [3].

Recently, different V-Ce-O oxide catalysts have been prepared in order to be used in the catalytic oxidation of diesel soot particles [4]. The combination of different physicochemical techniques has allowed us to define the nature of different vanadium oxide species present in the V-Ce-O compounds calcined at different temperatures from 400 to 800°C. In the temperature range of 400–550°C, polymeric V-O-V chains highly interacting

*Author to whom all correspondence should be addressed.
0022-2461
DOI: 10.1007/s10853-006-3160-3

with ceria surface are identified for low vanadium content. With the increase of the vanadium content vanadium tetrahedral surface species and then the V_2O_5 phase are evidenced in temperature range of 400–450°C. When the solids are heated at high temperatures (≥500°C), the formation of the $CeVO_4$ phase occurs from the reaction between V_2O_5 and CeO_2 oxides. Consequently, a single electron is trapped in an oxygen vacancy and can be considered as a probe to the $CeVO_4$ phase presence [5].

The determination of the nature of vanadium species can provide useful information leading to a better understanding of the elementary steps of heterogeneously catalyzed reactions. In fact, the basic steps of catalytic oxidation processes at the surface of metal oxides consist in redox interactions involving the solid and one or more reactants leading to the partial reduction of the catalyst. By the end of the catalytic oxidation of diesel soot particles, the catalyst is re-oxidized and finds back its initial oxidation state showing the influence of the vanadium species nature [6]. In this order, the redox properties of the identified vanadium species are simultaneously investigated by Temperature Programmed Reduction (TPR) and Electron Paramagnetic Resonance (EPR).

2. Experimental

2.1. Solids preparation

Ceria (CeO_2) was prepared by precipitation of cerium hydroxide from $Ce(NO_3)_3,6H_2O$ with a NaOH solution as described in [7]. The solid was calcined at 500°C for four hours under a flow of dried air. Subsequently, a solution of vanadyl oxalate VOC_2O_4 was impregnated on ceria to prepare xV10Ce samples with different V/Ce atomic ratios (x = 1.08, 1.67, 2.73 and 5.06), deduced from chemical analysis [5]. After drying at 100°C, the solids freshly prepared were calcined at 500°C under a flow of dried air for 4 h.

2.2. Temperature programmed reduction/oxidation (TPR/TPO)

Temperature Programmed Reduction (TPR) measurements were performed on a NETZSCH STA 409 apparatus. About 100 mg of calcined samples at 500°C (xV10Ce500) or reference compounds (CeO_2, V_2O_5 and $CeVO_4$) were considered and placed in a Al_2O_3 crucible. All solids were first treated under dried air at 300°C for one hour and then cooled to 20°C in order to eliminate the physisorbed water due to ambient humidity. The TPR results were corrected with respect to the weight loss corresponding to water departure. The temperature of the samples was raised at a rate of 5°C min^{-1} from 50 to 950°C under a flow (75 mL·min^{-1}) of 10 vol% H_2 in N_2. The exploitation of the weight losses has permitted to evaluate the reducibility properties of such samples in these conditions.

After reduction, all samples were re-oxidized under a mixture of 10 vol% O_2 in N_2. Temperature Programmed Oxidation (TPO) measurements were performed in the same conditions as above (apparatus, temperature rate, gas flow . . .).

2.3. Electron paramagnetic resonance (EPR)

The Electron Paramagnetic Resonance (EPR) measurements were performed at −269°C on a EMX BRUKER spectrometer with a cavity operating at a frequency of ∼9.5 GHz (X band). The magnetic field was modulated at 100 kHz. The g values were determined from precise frequency and magnetic field values. For EPR measurements, the samples were placed in a micro-flow reactor and treated under a flow (75 mL.min^{-1}) of 10 vol% H_2 + 90 vol%N_2 in the same conditions as above. The micro-flow reactor was assembled with an EPR quartz tube into which the catalyst could be transferred under the same atmosphere.

3. Results and discussion

3.1. Temperature programmed reduction

The redox properties of the V-Ce-O catalysts, associating the oxidation states Ce^{4+}/Ce^{3+} and V^{5+}/V^{4+}, have been then investigated by TPR. The TPR profiles of the xV10Ce500 samples (x = 1.08; 1.67 and 2.73) are shown in Fig. 1. Corresponding thermo-gravimetric (TG) measurement values are in Table I.

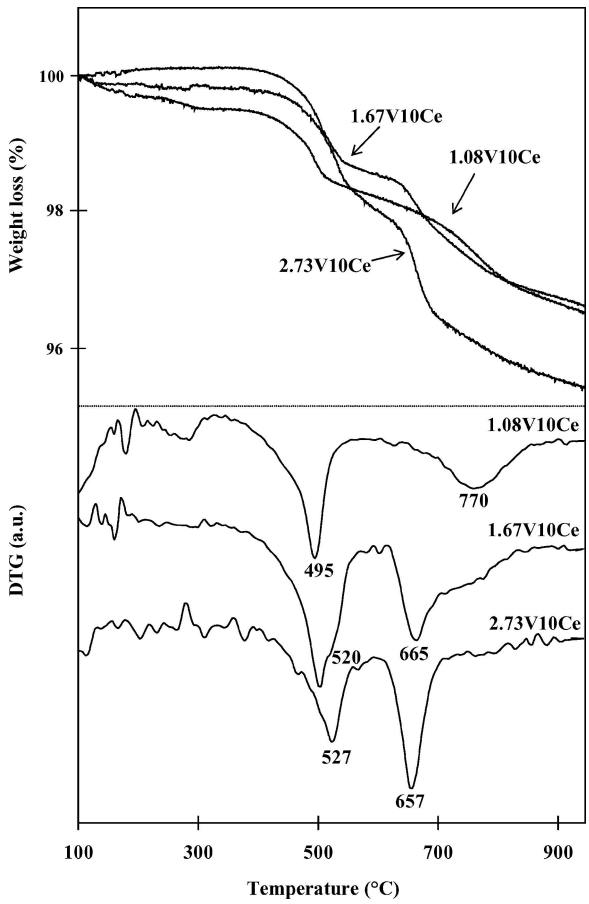

Figure 1 TG and DTG curves obtained over the TPR of the xV10Ce500 samples.

TABLE I Experimental and theoretical weight losses (%) obtained from the TPR measurements

Sample		400°C ≤ T ≤ 600°C		600°C ≤ T ≤ 730°C		T≥700°C	
		$V_2O_5 \rightarrow 2VO$		$CeVO_4 \rightarrow CeVO_3$		$2CeO_2 \rightarrow Ce_2O_3$	
	Total loss	Theoretical	Experimental	Theo	Exp	Theo	Exp
1.08V10Ce	3.040	1.425	1.420	–	–	4.397	1.620
1.67V10Ce	3.510	1.521	1.520	0.412	0.414	4.073	1.576
2.73V10Ce	4.380	1.772	1.770	1.045	1.047	3.558	1.563

TABLE II Composition of *x*V10Ce500 samples as a combination of V_2O_5, $CeVO_4$ and CeO_2 oxides, deduced from chemical and spectroscopic analysis

Sample	Atomic composition	Weight composition		
		V_2O_5	$CeVO_4$	CeO_2
1.08V10Ce500	$(V_2O_5)_{0.54}(CeO_2)_{10}$	5.41%	–	94.59%
1.67V10Ce500	$(V_2O_5)_{0.593}(CeVO_4)_{0.484}(CeO_2)_{9.516}$	5.77%	6.60%	87.63%
2.73V10Ce500	$(V_2O_5)_{0.723}(CeVO_4)_{1.284}(CeO_2)_{8.716}$	6.72%	16.72%	76.56%
5.06V10Ce500	$(V_2O_5)_{1.720}(CeVO_4)_{1.620}(CeO_2)_{8.380}$	14.44%	19.06%	66.50%

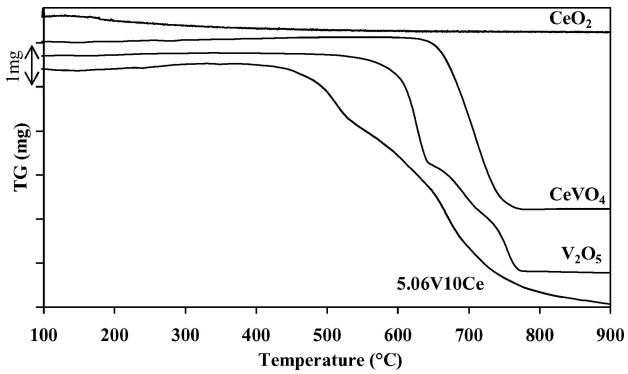

Figure 2 TG curves obtained over the TPR of CeO_2, V_2O_5, $CeVO_4$ and 5.06V10Ce500 samples.

TABLE III Experimental and theoretical weight losses (%) obtained from the progressive reduction of V_2O_5

Reaction	Temperature	Experimental loss	Theoretical loss
$V_2O_5 \rightarrow V_6O_{13}$	625°C	5.84	5.86
$V_6O_{13} \rightarrow VO_2$	640°C	2.93	2.93
$VO_2 \rightarrow V_5O_9$	710°C	3.53	3.51
$V_5O_9 \rightarrow V_2O_3$	775°C	5.23	5.28

For all the samples, different weight losses were reported: the first one started slightly above 400°C and is clearly observed in the range of 490–530°C, the second, evidenced at higher temperature (600°C $< T <$ 730°C) depends on the vanadium content in the samples. Indeed, a weight loss is observed at 665°C for 1.67V10Ce and occurs at 657°C for 2.73V10Ce. Finally, a continuous weight loss, clearly observed for the 1.08V10Ce sample in the range of 770°C, is evidenced on the TG curves, for all the *x*V10Ce samples, until 950°C. In order to have a reliable attribution of these different phenomena, CeO_2, V_2O_5 and $CeVO_4$ oxides have been investigated by TPR (Fig. 2).

The presence of these latter oxides in the *x*V10Ce500 samples have been highlighted in a previous work [5] where each *x*V10Ce500 solid could be considered as a combination of these three oxides in different proportions (Table II). These data have been deduced from the combination of chemical and spectroscopic analysis (^{51}V MAS NMR, Raman, XRD . . .) [5].

The CeO_2 oxide calcined at 500°C and used as support for the xV10Ce samples is not affected by the reducing conditions of the TPR treatment (Fig. 2). However, literature data [8] clearly show surface and bulk reduction of ceria at ∼500°C and ∼850°C respectively. Theoretical weight loss related to the total reduction of ceria into Ce_2O_3 should be 4.65%. The behavior observed in our case can be related to the residual alkaline cations resulting from the preparation method of the CeO_2 support. In fact, the presence of these cations has been revealed by the chemical analysis (320 ppm of sodium) while the calcination treatment induces their migration to the solid surface [7]. This alkaline layer would protect the ceria surface from reduction by H_2.

The reduction of V_2O_5 to V_2O_3 is evidenced between 600° and 790°C and proceeds in several steps, the intermediate species being V_6O_{13}, VO_2 and V_5O_9 where the total weight loss is 17.58%. Experimental and theoretical weight losses associated to different reduction steps are reported in Table III.

These data are in agreement with those observed in literature showing the reduction of V_2O_5 into V_2O_3 in this range of temperature [9]. Nevertheless, the impurities content, the preparation method and the partial pressure of hydrogen can have major influence on the reduction level of vanadium oxide. Generally, the reduction of V_2O_3 into VO is observed over a temperature of 1000°C.

Finally, $CeVO_4$ phase is reduced in one step at 705°C. The mass loss of 6% obtained during this reduction can be due to the formation of $CeVO_3$ in agreement

with theoretical weight loss (6.27%) and literature data [10].

Concerning the first weight loss observed in the range of 400–600°C for the *x*V10Ce500, the theoretical values, deduced from the composition of the sample (Table II) and the reduction of V_2O_5 into V_2O_3, are always smaller than the experimental losses. Thus, the possibility of a more pronounced reduction of V_2O_5 into VO is considered and the resulting theoretical losses are reported in Table I. These values are in perfect agreement with the experimental losses measured from the TG curves which confirm the reduction of V_2O_5 into VO. In addition, the TPR results clearly show that the polymeric V-O-V chains (1.08V10Ce) are more easily reducible than V_2O_5 phase. However, it is already demonstrated that the increase of the vanadium content leads to a decrease of the "vanadium species—ceria support" interaction [5]. Thus, similar to palladium and copper supported on ceria [8, 12, 13], the V_2O_5-CeO_2 interaction facilitates the reduction of the vanadium species. For higher vanadium loading, 1.67V10Ce, 2.73V10Ce and 5.06V10Ce, the V_2O_5-CeO_2 are more easily reducible than pure V_2O_5 oxide (Figs 1 and 2).

The second mass loss (Table I) increases with the increasing of the vanadium content and can be attributed to the reduction of $CeVO_4$ phase, present in the solids, into $CeVO_3$. In fact, this $CeVO_4$ phase is missing in the 1.08V10Ce500 sample (Table II) which explains the absence of the weight loss in the temperature range of 600–730°C in this case (Fig. 1, Table I). In addition, the reduction temperatures are shifted towards smaller values with the increase of the vanadium content (Figs 1 and 2). The presence of a trapped electron nearby the $CeVO_4$ phase [5], the VO and CeO_2 oxides would facilitate the reduction of $CeVO_4$ into $CeVO_3$.

In all the cases (*x*V10Ce500) and on the contrary of pure oxides (Figs 1 and 2), a continuous weight loss is observed until 950°C. In addition, the total experimental weight loss is considerably higher than the theoretical values corresponding to the reduction of V_2O_5 and $CeVO_4$. Thus, a partial reduction of the CeO_2 support is evidenced (Table I) for all the *x*V10Ce500 samples treated in these conditions. Indeed, partial reduction of ceria has been observed in presence of precious metal by a spillover process [14]. In addition, it is well known that dissociative adsorption of hydrogen on vanadium does not take place easily at low temperature. However, in our case the possibility that the partial reduction of ceria occurs versus hydrogen spillover should not be omitted. This result is in good agreement with literature data where a partial reduction of ceria during metal cations reduction, has been observed [8, 12–14]. Finally, it is important to note that, contrary to CeO_2 reference sample, the presence of sodium seems to be unable to protect ceria from reduction via a vanadium spillover process.

3.2. Electron paramagnetic resonance

The general redox properties of a metal oxide can be investigated by means of the electron paramagnetic resonance technique which is capable of detecting the paramagnetic centers often formed upon one electron redox processes. In fact, EPR offers a powerful and sensitive technique for investigating the oxidation states, surface and bulk co-ordination and the physical form of a transition metal oxide. EPR technique has been extensively used to characterize supported vanadia systems in order to elucidate the nature of the paramagnetic species, their local structure and the effect of the active phase — support interaction [15].

EPR spectra of ions with $S > ½$ and $I \neq 0$ may be analyzed using an axial symmetry H spin-Hamiltonian:

$$\begin{aligned}\mathcal{H} = {} & g_{//}\beta H_z S_z + g_\perp \beta \left(H_x S_x + H_y S_y\right) \\ & + A_{//} I_z S_z + A_\perp \left(I_x S_x + I_y S_y\right) \\ & + D\left[S_z^2 - \frac{1}{3}S(S+1)\right] + E\left(S_x^2 - S_y^2\right) \quad (1)\end{aligned}$$

where D and E are the crystal-field parameters, S and I denote the total electron and nuclear spins, g is the g-factor and A is the Hyper Fine Structure (HFS) constant. In the case of $S = ½$, $D = E = 0$.

Fig. 3 shows the EPR spectra, recorded at −269°C, obtained before and after the reduction of the 1.08V10Ce500 sample. For the calcined sample, the EPR spectrum is the superimposition of two signals with $g < 2$ denoted by A and B and described elsewhere [5, 7]. The A and B signals are characterized by $g_{xx(A)} = 1.9654$, $g_{yy(A)} = 1.9626$, $g_{zz(A)} = 1.9398$ and $g_{xx(B)} = 1.9692$, $g_{yy(B)} = 1.9670$, $g_{zz(B)} = 1.9465$ and attributed to the presence of two different Ce^{3+} (f^1 ions; $g_e > g_\perp > g_{//}$) sites in the solid or more precisely to an interaction between conduction electrons and 4f orbital of Ce^{4+} ions in the CeO_2 matrix. These signals are also present on the EPR spectrum of the ceria support before impregnation. The A signal has been attributed to Ce^{3+} species with easily removable ligands and the B signal to Ce^{3+} ions stabilized by some lattice defects CeO_{2-x} [7]. Finally, it is important to notice that no signal relative to V(IV) species is observed indicating that the totality of the vanadium species are in V(V) oxidation state.

The EPR signal at $g = 4.27$ (Fig. 3) is the well-known EPR transition for Fe^{3+} ions; electronic configuration ($3d^5$). This spectrum is characteristic of high spin Fe^{3+} ions (ground state $^6S_{5/2}$), located in octahedral or tetrahedral [16] co-ordination sites having a strong rhombic distortion of the crystal field. Indeed, if in equation (1) where $S = 5/2$ and $I = 0$ (since the natural abundance of the ^{57}Fe isotope ($I = ½$), is only of 2.15%) the terms of the crystalline field have the same values as the Zeeman term or are larger (D, $E \geq g\beta H$), the spectral

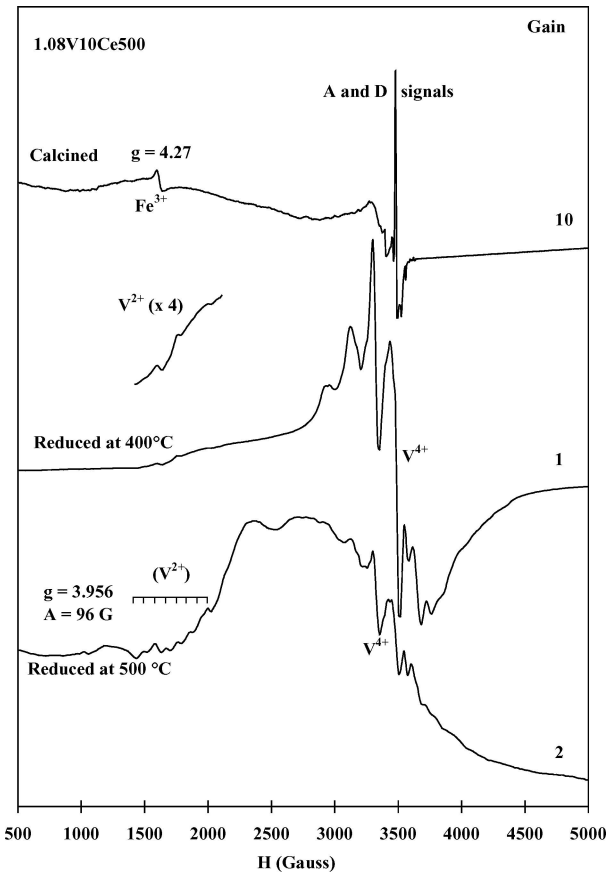

Figure 3 EPR spectra recorded at −269°C for the 1.08V10Ce500 sample at different temperatures of reduction treatment.

features are strongly affected by the relative magnitudes of the coefficients D and E. In the case of a "purely rhombic" ligand field, $|E/D| = 1/3$, an isotropic signal at $g = 4.27$ is observed. The line with $g = 4.27$ is due to transitions within the middle Kramers doublet [17–21]. The lower and upper doublets exhibit strongly anisotropic values of effective g-factors which give rise to very low intensity of corresponding EPR transitions in poly-crystalline solids. Fe^{3+} ions should be considered as impurities in the solid.

When reduced at 400°C the EPR spectrum of the 1.08V10Ce500 sample exhibits different EPR signals. It consists of several independent EPR spectra due to different paramagnetic species. The most intense part of the spectrum has been attributed earlier [22] to two sites of V^{4+} ($3d^1$) characterized by EPR parameters in equation (1) with $S = 1/2$ and $I = 7/2$ (99.76% of ^{51}V natural abundance with nuclear spin $I = 7/2$). Site $_{(1)}$ $g_{||} = 1.923$, $A_{||} = 174$ G; $g_{\perp} = 2.000$, $A_{\perp} = 76$ G, $g_{iso} = 1.974$, $A_{iso} = 109$ G and site $_{(2)}$ $g_{||} = 1.890$, $A_{||} = 205$ G; $g_{\perp} = 2.000$, $A_{\perp} = 76$ G, $g_{iso} = 1.963$, $A_{iso} = 119$ G. In the case of isolated V (IV) species, information about their environment can be obtained from g and A values. These could correspond to VO^{2+} ions in octahedral symmetry axially distorted since $1.955 < g_{iso} < 1.980$ and $80\ G < A_{iso} < 120\ G$ [23]. Generally, lower g_{iso} and A_{iso} values are expected in the cases of V^{4+} species in octahedral symmetry $1.920 < g_{iso} < 1.950$ and $60\ G < A_{iso} < 90\ G$ [24–26].

The second EPR signal is centered at $g = 3.956$ and exhibits eight well-resolved HFS lines with $A = 96$ G. This EPR signal is also due to vanadium ions and could be attributed to the perpendicular components of one of the fine transitions corresponding to the V^{2+} ($3d^3$) spectrum. The theoretical estimation of the EPR parameters from equation (1) with $S = 3/2$ and $I = 7/2$ within the limits of strong axial crystal field ($g\beta H << D$) gives rise to axial symmetry spectrum with $g_{||} \approx 2$ and $g_{\perp} \approx 4$ [27]. This prediction is in good agreement with the experimental results found in the literature [28]. The $g_{||} \approx 2.0$ component cannot be seen in our case because of the large V^{4+} spectra intensities situated just in the range of $g = 2.0$. Moreover, the intensity of the parallel lines in an anisotropic spectrum is generally weaker than that of perpendicular ones.

Theoretically, the EPR signal at $g = 3.956$ could also be due to two other types of vanadium paramagnetic centers. It could be interpreted:

(i) as a forbidden ($\Delta M_s = \pm 2$) transition of a pair V^{4+}-V^{4+} ($S = 1$; $I = I_1 + I_2 = 7$) [25]; however, in this case, 15 (and not 8) HFS lines ($2I + 1$), with the binomial intensity distribution, should be observed,

(ii) as the same type of the forbidden transition of V^{3+} ($S = 1$; $I = 7/2$), but, regarding this possibility, literature data confirm that it is unusual to observe V^{3+} ions because such species are not stable. Their EPR spectra can be mainly recorded at −269°C and at high frequency [28]. Moreover, in earlier works, this forbidden transition ($\Delta M_s = \pm 2$) of V^{3+} ions has never been observed at $g = 3.956$ because of the strong zero field splitting [28].

It should be important to notice that in our case, the 8 lines centered on $g = 3.956$ have been observed either at −269°C, −196 C or at room temperature [22].

For a reduction temperature of 500°C, the intensity of the EPR signal centered at $g = 3.956$ increases whereas, that of the signal corresponding to V^{4+} species decreases. These results are in perfect agreement with those reported in the TPR part of this work. Indeed, at this temperature of reduction (500°C) for the 1.08V10Ce500 sample, the major part of the vanadium species is present as VO oxide (Fig. 1).

The EPR spectrum of the calcined 2.73V10Ce500 sample (Fig. 4) shows, in addition to the Fe^{3+} ions ($g = 4.27$), two EPR signals in the region of $g < 2$. The first is an isotropic signal with $g = 1.964$ and a line width of $\Delta H = 100$G superimposed with a second one presenting a very bad resolution of a HFS making impossible the determination of the EPR parameters. Nevertheless, these signals can be attributed to V^{4+} species or trapped electrons nearby vanadium atoms during the calcination of the solid [23].

When reduced at 400°C the EPR spectrum of the 2.73V10Ce500 sample exhibits the same EPR signals, in the range of g ≈ 2, observed for the 1.08V10Ce500 sample and assigned to VO^{2+} ions in octahedral symmetry axially distorted. On the contrary, the V^{2+} EPR signal (g = 3.956) is not observed in this case confirming our TPR results. In fact, with the increase of the vanadium content in the samples, the reduction of the vanadium species proceeds at higher temperature. In this order, the 2.73V10Ce500 sample is reduced at 550°C (Fig. 4) with respect to the TPR data showing the reduction of the vanadium species at a temperature of 527°C (Fig. 1). A signal with $g = 3.956$ and $\Delta H = 652$G is observed and can be attributed to the V^{2+} ions. However, in this case, the vanadium content is considerably higher leading to the formation of agglomerates which increases the dipolar interaction and consequently the broadness of the EPR lines.

An other signal centered at g = 1.977 ($\Delta H = 95$G) can be related to the presence of small agglomerates of V^{4+} in the solid. With the increase of the reduction temperature (600°C) the width ($\Delta H = 72$G) and the intensity of this signal decrease (Fig. 4) indicating the reduction of the V^{4+} ions. In parallel, the EPR signal relative to V^{2+} ions is not observed which could be explained by high dipolar

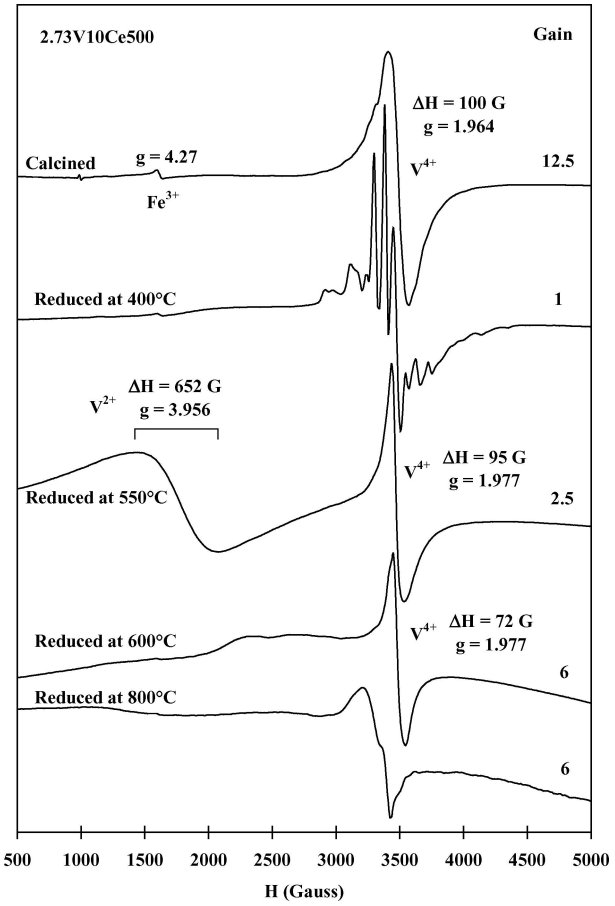

Figure 4 EPR spectra recorded at −269°C for the 2.73V10Ce500 sample at different temperatures of reduction treatment.

TABLE IV Reduction and oxidation temperatures corresponding to V_2O_5 species interacting with ceria in the *x*V10Ce500 samples.

Sample	Reduction Temperature	Oxidation Temperature
V_2O_5 (ref.)	600°C < T < 800°C	200°C < T < 475°C
1.08V10Ce500	495°C	> 500°C
1.67V10Ce500	520°C	~500°C
2.73V10Ce500	527°C	445°C
5.06V10Ce500	~550°C	410°C

interactions leading to a large line width of the signal, mixed up with the base line of the spectrum. For a reduction temperature of 800°C, the EPR spectrum is the result of the superimposition of different EPR signal relative to V^{2+}, V^{3+} and Ce^{3+} which makes the assignment of the EPR lines very hazardous. Indeed, at this temperature the TPR results show the simultaneous presence of the VO, $CeVO_3$ and Ce_2O_3 oxides.

3.3. Temperature programmed oxidation

When active phase is involved in redox process as in the case of catalytic diesel soot oxidation, fast re-oxidation of the catalyst is necessary to maintain a high catalytic reactivity. In fact, catalytic results have shown that vanadium and cerium oxides are the active phases whereas $CeVO_4$ oxide is inactive towards the diesel soot oxidation reaction [6]. In addition, cerium compounds are used as promoting additives for diesel soot combustion and ceria is a well-known catalyst for such reaction [29, 30]. Thus, the aim of this part of the study is to compare the redox behavior of the different vanadium species present in the *x*V10Ce500 samples. Table IV summarizes the reduction and oxidation temperatures corresponding to $V_2O_5 \rightleftarrows VO$ species interacting with ceria. From these results we can conclude that polymeric V-O-V chains are easily reducible but hardly re-oxidized. On the contrary, V_2O_5 species present in the high vanadium loading samples are hardly reducible but easily re-oxidized at temperatures < 500°C (Table IV). Further investigations by ^{51}V MAS NMR, Raman and XRD have shown that these processes are reversible. However, the proportions of each oxide (V_2O_5, CeO_2 and $CeVO_4$) in the solids are faintly affected by the redox cycle showing a slight increase of $CeVO_4$ phase which can be explained by the high temperatures of reduction and re-oxidation treatments [4, 5, 11]. These results would be of major importance to enlighten the catalytic behavior of these solids versus the combustion reaction of diesel soot particulate [6].

4. Conclusion

The redox properties of V-Ce-O oxides have been simultaneously investigated by TPR/TPO and EPR techniques. Main information is deduced about the redox behavior of the different vanadium species in the samples. Thus, polymeric V-O-V chains and V_2O_5 species are more

easily reducible than the $CeVO_4$ phase. The reduction of pure V_2O_5 to V_2O_3 proceeds in several steps, the intermediate species being V_6O_{13}, VO_2 and V_5O_9. The reduction of V_2O_5 species interacting with ceria support leads to VO oxide. EPR measurements performed at $T = -269°C$ have permitted to observe progressively different signals of V^{4+} in addition to vanadium ions in V^{2+} ($3d^3$) paramagnetic configuration. This attribution is based on an EPR signal at $g = 3.956$ with eight well resolved hyper fine lines ($A = 96$ Gauss), which may be attributed to the perpendicular components of one of the fine transitions corresponding to the V^{2+} spectrum. At high reduction temperature, $CeVO_4$ phase leads in one step to $CeVO_3$ and a continuous and partial reduction of CeO_2 into Ce_2O_3 is observed. Re-oxidation process shows that polymeric V-O-V chains, easily reducible, are hardly re-oxidized whereas V_2O_5 species, present in the high vanadium loading samples, are easily re-oxidized at low temperatures. These results would be of major importance to explain the catalytic behavior of these solids versus the combustion reaction of diesel soot particulate.

Acknowledgments

The authors would like to thank the "Région Nord — Pas de Calais" and the European Community (European Regional Development Fund) for financial support

References

1. A. F. AHLSTRÖM and A. ODENBRAND, *Appl. Catal.* **60** (1990) 157.
2. L. LIETTI and P. FORZATTI, *J. Catal.* **147** (1994) 241.
3. R. KORNER, N. RICKEN and I. RIESS, *J. Sol State Chem.* **78** (1989) 136.
4. J. MATTA, E. ABI-AAD, D. COURCOT and A. ABOUKAÏS, *J. Therm. Anal. Calorim.* **66** (2001) 717.
5. J. MATTA, D. COURCOT, E. ABI-AAD and A. ABOUKAÏS, *Chem Mater.* **14** (2002) 4118.
6. J. MATTA, E. ABI-AAD, D. COURCOT and A. ABOUKAÏS, *to be published.*
7. E. ABI-AAD, R. BECHARA, J. GRIMBLOT and A. ABOUKAÏS, *J. Chem. Soc. Faraday Trans.* **5** (1993) 793.
8. C. DECARNE, E. ABI-AAD, B. G. KOSTYUK, V. V. LUNIN and A. ABOUKAÏS, *J. Mater. Sci.*, **39** (2004) 2349 and references therein.
9. F. ROOZEBOOM, M. C. HAZELEGER, J. A. MOULIJN, J. MEDEMA, V. H. J. DE BEER and P. J. GELLINGS, *J. Phys. Chem.* **84** (1980) 2783.
10. H. YOKOKAWA, N. SAKAI, T. KAWADA, and M. DOKIYA, *J. Am. Ceram. Soc.* **73** (1990) 649.
11. R. COUSIN, D. COURCOT, E. ABI-AAD, S. CAPELLE, J-P. AMOUREUX, M. DOURDIN, M. GUELTON and A. ABOUKAÏS, *Coll and Surf, A* **158** (1999) 43.
12. C. BINET, A. JADI, J. C. LAVALLEY and M. BOUTONNET-KIZLING, *J. Chem. Soc. Faraday Trans.* **88**(14) (1992) 2079.
13. L. KUNDAKOVIC and A. FLYTZANI-STEPHANOPOULOS, *Appl. Catal. A: General* **171** (1998) 329.
14. H. C. YAO and Y. F. YU YAO, *J. Catal.* **86** (1984) 254.
15. E. GIAMELLO, *Catal. Today* **41** (1998) 239.
16. C. M. BRODBECK and R. R. BUKREY, *Phys. Rev.* **24** (1981) 2334.
17. D. L. GRISCOM, *J. Non Cryst. Solids* **40** (1980) 211.
18. J. M. SCHREURS, *J. Chem. Phys.* **69** (1978) 2151.
19. R. D. DOWSING and J. F. GIBSON, *ibid.* **50**(**1**) (1969) 294.
20. E. A. ZHILINSKAYA and V. N. LAZUKIN, *J. Non-Cryst. Solids* **50** (1982) 163.
21. V. N. LAZUKIN, I. V. CHEPELEVA, E. A. ZHILINSKAYA and A. P. CHERNOV, *Phys. Stat. Sol. B* **69** (1975) 399.
22. E. ABI-AAD, A. BENNANI, J.-P. BONNELLE and A. ABOUKAÏS, *J. Chem. Soc. Faraday Trans.* **914** (1995) 99.
23. E. ABI-AAD, D. COURCOT, A. ABOUKAÏS, M. BAERNS, A. BRUCKNER, M. GUELTON and J. C. VEDRINE, *Catal. Today* **56** (2000) 371.
24. A. DAVIDSON and M. CHE, *J. Phys. Chem.* **96** (1992) 9906.
25. L. D. BOGOMOLOVA, A. N. KHABAROVA, E. V. KLIMASHINA, N. A. KRASILNIKOVA and V. A. JACKIN, *J. Non Cryst. Solids* **103** (1988) 319.
26. G. CENTI, S. PARATHONER, F. TRIFIRO, A. ABOUKAÏS, C. F. AÏSSI and M. GUELTON, *J. Phys. Chem.* **96** (1992) 2617.
27. G. M. ZHIDOMIROV, *Interpretation of Complex EPR Spectra* Nauca, Moscow (1975) .
28. E. ABI-AAD, E. A. ZHILISKAYA and A. ABOUKAÏS, *J. Chim. Phys.* **96** (1999) 1519 and references therein.
29. E. ABI-AAD, R. COUSIN, C. PRUVOST, D. COURCOT, C. RIGAUDEAU, R. NOIROT and A. ABOUKAÏS, *Topics in Catalysis* **16/17** (2001) 263.
30. R. FLOUTY, E. ABI-AAD, S. SIFFERT and A. ABOUKAÏS, *Appl. Catal. B* **46** (2003) 145.

Received 23 April 2004
and accepted 14 April 2005